SIMPLE CALIBRATION TECHNIQUES FOR NON-METRIC CAMERAS

George E. Karras, Dionyssia Mavrommati
Department of Surveying, National Technical University of Athens
GR-15780 Athens, Greece (e-mail: gkarras@central.ntua.gr)

KEY WORDS: non-metric cameras, interior orientation, lens distortion, camera calibration, bundle adjustment, rectification

ABSTRACT
Architectural documentation is carried out mostly with (analogue or digital) non-metric cameras or video-cameras. Unknown internal geometry is a main problem in this context, particularly for wide-angle lenses with their considerable amount of distortion. Self-calibrating bundle adjustment or 3D test-field calibration may provide straightforward answers to this problem, yet on occasions such steps can prove too complicated or costly for ordinary users. Hence, this paper discusses the use of simple pre-calibration approaches.

Practical examples with wide-angle lenses are first given to illustrate that, in general, use of "nominal" values for the camera constant and the principal point causes no significant problem in most cases of low or moderate accuracy requirements. These same examples, however, reveal the marked effects of radial distortion. This is a main problem which needs to be controlled, even in the simple and most popular among users method of rectification (for which knowledge of the primary interior orientation parameters is irrelevant). Here, simple approaches for determining radial distortion are presented and assessed, ranging from the use of linear features on man-made objects to rectification of regular grids and its various alternatives. On the other hand, the easiest approach for full camera calibration is probably by the common adjustment of images of targeted 2D objects taken under different viewing angles. In the results given the described methods for determining radial distortion have also been evaluated. In conclusion, both the merits and limitations of the discussed simple calibration techniques are outlined but also a gross distinction between analogue and digital camera is made.

1 INTRODUCTION

It is a common experience that most of today's photogrammetric applications in architectural and archaeological documentation are carried out by means of non-metric cameras, either analogue or digital. This holds true not only regarding published projects but also encompasses those numerous unpublished cases in which non-metric images are applied on a routine basis by individual users, firms or public services in the course of everyday documentation tasks. Understandably enough, such a "metric" use of non-metric cameras (made possible by the analytical and digital photogrammetric as well as image processing tools) is very popular among non-expert users, namely architects, archaeologists, restorers, conservationists but also engineers. This possibility of using non-metric cameras is a decisive factor for what has been called the "democratisation of photogrammetry".

But speaking of an ordinary amateur camera almost automatically raises the matter of its internal geometry or its interior orientation. Indeed, many questions of non-experts revolve about this point. On the other hand, numerous camera types available on the market could be employed, and in fact are employed, for documentation and conservation purposes. To this one should add the fact that (perhaps contrary to the wishes of some photogrammetrists…) a significant number of applications in archaeology or architecture pose moderate, or even low, accuracy requirements. In this context, the following (rhetorical) questions arise:

- is every user expected to calibrate a camera?
- and for all tasks?
- and every camera?

In the photogrammetric literature and practice there exist several alternatives regarding how to handle the problem of interior orientation. Here, the following approaches could be mentioned:

Use of a projective approach. The use of projective equations, whenever possible, frees users from the need to know the interior orientation parameters of their camera. These are the cases of 2D-2D rectifications or of the 2D-3D direct linear transformation (DLT). The first technique, a very popular practical tool, is inherently limited to (nearly) planar objects, while the second generally requires geodetic control with sufficient extension in depth. And, of course, the problem of lens distortion, which causes non-projective image deformations, remains.

Test-field calibration. This is the conventional camera calibration approach, but it evidently implies that users have to construct (and maintain) an accurate targeted 3D test-field, designed for all cameras, lenses and focusing distances they will use.

Bundle adjustment solutions. In principle, a geometrically sound bundle adjustment will produce good results for the particular application. However, unless performed in strictly controlled environments, different adjustments can yield strongly diverging values for the interior orientation elements. Thus, one cannot simply accept any solution as the definite values for the camera parameters.

Other simpler techniques. Among such calibration alternatives, use of image vanishing points is mentioned. Here again, acceptable results can be expected for the particular images used (for instance, historic photographs of destroyed buildings). Yet, the repeatability of such techniques is generally rather poor, and they could not be regarded as general-purpose calibration methods.

Further to this, a fundamental question concerns the image coordinate system itself of analogue amateur cameras. Generally "fixed" through the four corners of the negative, the image system is indeed very poorly defined. This clearly has a direct impact upon the reproducibility of the image principal point. Thus, in most cases one may ask: is it meaningful to attempt and estimate a deviation from an "ideal" image centre if the location of this centre may be uncertain to an extent comparable to, or even larger than, the deviation itself? This consideration illuminates the following choice regarding interior orientation often adopted in practice.

2 "NOMINAL" INTERIOR ORIENTATION AND THE EFFECT OF DISTORTION

It often happens that, in many cases of moderate and low accuracy requirements, the principal points is simply ignored and the value of the focal length *f* is used as the camera constant *c*. Clearly, this presupposes that, first, a "nominal" f does exist (which is not the case with certain cameras for which no information is available either about f and/or about image format), and that focusing is at infinity; and second, that the camera is not regarded as a "shift" camera, and additionally that the whole negative format is used. Under these circumstances, analogue cameras can yield acceptable results for several tasks as illustrated in the following examples.

- Example 1: Project "Sparta" (Fig. 1)

This example is drawn from a recent photogrammetric project regarding the parodoi of the Ancient Theatre of Sparta (Petsa, 2001). The strip used here consists of 8 images, acquired with a medium format 60x45mm^2 Mamiya camera with a wide-angle 45 mm lens using a fishing-rod to raise the camera. Mean image scale was ~ 1:300 and 40 natural detail control points were used. The object had a considerable extension ΔH in depth which reached maximally up to 20% of the mean imaging distance H.

Figure 1: Project "Sparta": footprints of the image strip and corresponding part of the final orthoimage

Starting from "nominal" values for the inner orientation elements (c, x_o, y_o) and a radial distortion curve estimated as outlined in 3.1, a test was carried out by modifying c, x_o, y_o and repeating the bundle adjustment. Fig. 2 shows the RMS values for the control points.

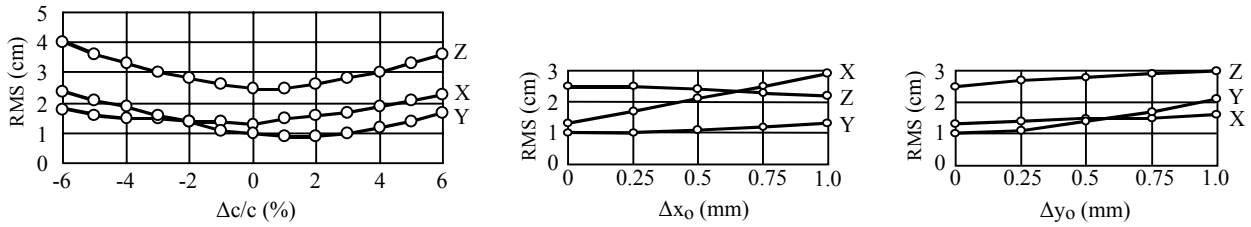

Figure 2: Project "Sparta": variation of RMS control points errors with changing values of the interior orientation parameters

The above results point to the known fact that very large changes of the camera constant c lead to considerable errors. However, the loss in accuracy appears here as negligible for changes of c up to 1-2%, which already represent a rather large tolerance (it is not expected that it will be exceeded in most practical applications). Furthermore, changes in the x or y position of the principal point have a marked effect primarily upon the object coordinates in the same direction, with x_o errors having the strongest effect in X (direction of the strip). Here again, however, a "reasonable" deviation of 250 μm or even 500 μm could be tolerated in many practical tasks.

Clearly, it is not feasible to formulate tolerance limits valid for the multiplicity of cases met in practice. On a general level, however, the tolerances for interior orientation depend mainly on the opening angle of the camera and the depth extension of the object (Kölbl, 1976). When object depth increases with respect to the imaging distance the errors of interior orientation are decreasingly "absorbed" by the elements of exterior orientation. This could cause severe problems in instances with extreme variations in 3D but is far less annoying in cases concerning "flatter" objects (Galinou and Katsali, 2000).

- Example 2: Project "Omorfoklissia" (Fig. 3)

This case is taken from a work concerning a small but beautiful and important Byzantine church in Athens (Bieler et al., 2001).

Figure 3: Project "Omorfoklissia": four of the 22 images used in the adjustment

The all-around coverage of the monument was achieved using two cameras and three lenses, namely the medium format Mamiya camera with the wide-angle 45 mm and a normal 80 mm lenses, and a small format Nikon camera (wide-angle 28 mm lens) which was raised for taking tilted images. In the bundle adjustment, performed with the commercial software *Pictran*, a total of 8 control points were used along with 11 constraints on geodetically measured distances, while 8 check points were also at hand. The radial distortion Δr of all three lenses was known beforehand, for the Mamiya lenses from test-field calibration, for the Nikkor lens from a previous bundle solution with the *Bingo* software (Karras et. al., 1999). Here, solutions with self-calibration are tested against those using the "nominal" interior orientation values, but also the effect of radial distortion is studied. The results are seen in Table 1.

Table 1. Self-calibration vs. "nominal" values and test on radial lens distortion Δr
cameras: 2, lenses: 3, images: 22, control points: 8, known distances: 11, check points: 8

Interior orientation	Correction of Δr	σ_o (mm)	RMS of check points (cm)		
			X	Y	Z
self-calibration	yes	2.4	0.7	0.8	0.5
use of nominal values	yes	3.6	0.8	1.0	0.5
self-calibration	no	8.1	1.7	2.4	1.1
use of nominal values	no	9.1	2.3	2.6	2.4

The last two rows show that, when radial distortion was ignored, self-calibration improved accuracy, at least in one dimension. However, the striking difference is between solutions with (first two rows) and without (last two rows) correction of Δr. In the first case, both self-calibration and use of "nominal" values for interior orientation gave significantly higher accuracy, with their results being practically identical. The present example, based on a large number of images and a combination of three lenses, indicates that the crucial factor is radial distortion rather than the three basic elements of interior orientation.

- Example 3: Project "Thisseio" (Fig. 4)

This last example is drawn from a project concerning an archaeological site in Athens (Karras et al., 1999).

Figure 4: Project "Thisseio": footprints of the image strip and final orthoimage

Here the site had been recorded with 12 low altitude balloon images using the same small format Nikon camera (f = 28 mm). Mean image scale was ~ 1:1100 and 88 natural detail control points were available (± 3 cm). The object surface displayed relatively small deviations from a best-fitting plane (~6% of the imaging distance). The influence of radial distortion was tested here both for this as well as for the previous project "Sparta". Results are presented in Table 2.

Table 2. Bundle adjustments with and without correction of radial lens distortion Δr

	Correction of Δr	RMS of control points (cm)		
		X	Y	Z
Project "Sparta"	yes	1.3	1.1	1.4
(8 images, 40 control points)	no	5.5	3.5	19.4
Project "Thisseio"	yes	3.8	4.6	3.3
(12 images, 88 control points)	no	6.0	6.7	10.2

These tests, too, witness a drastic deterioration of accuracy when radial distortion is ignored. One is led to the remark that, in general, such errors appear as being much more important than small errors in the camera constant and the principal point. Besides, as already mentioned, radial distortion needs anyway to be taken into account, even when projective equations (notably rectification) are used. Hence, techniques preferably simple are necessary for determining the radial distortion polynomial.

3 SIMPLE METHODS FOR ESTIMATING RADIAL LENS DISTORTION

Of course, radial symmetric lens distortion Δr can be determined in a common solution with the other interior orientation parameters (through test-field calibration or bundle adjustment) but may also be estimated separately. Such independent knowledge of the radial distortion of a lens is useful in a variety of cases, for instance:

- correction of image coordinates in rectification or for the DLT approach (whereby the coordinates must obviously refer to the image coordinate system)

- correction of image coordinates in cases, as those given previously, where "nominal" interior orientation values are used
- correction of image coordinates for test-field calibration or self-calibration algorithms which cannot recover Δr
- last but not least, for resampling digital images (rectified or otherwise) to free them from the distortion effect.

Radial symmetric lens distortion is expressed through the coefficients of a polynomial referring to the radial image distance r

$$\Delta r = k_o r + k_1 r^3 + k_2 r^5 \tag{1}$$

and is split into its x and y components as

$$\Delta x = \Delta r \frac{x}{r} = x\,(k_o + k_1 r^2 + k_2 r^4) \qquad \Delta y = \Delta r \frac{y}{r} = y\,(k_o + k_1 r^2 + k_2 r^4) \tag{2}$$

The first term in Eq. 1 is linear, i.e. is simply a scale factor, and cannot be estimated in all instances (e.g. in a full calibration process where the camera constant c also plays the role of a scale factor). Thanks to this connection with c, a distortion polynomial Δr may be transformed to a different form, which is coupled with a correspondingly modified value for c to describe the same central projection. Among the available criteria for transforming a Δr curve, it has been chosen here to give all polynomials in the form minimizing the sum of squares of Δr up to a maximal image radius (Karras et al., 1998).

3.1 Estimation of distortion from the curvature of straight lines

Straight lines can be used to estimate radial distortion, since the latter is the main reason for their curved appearance on the images. It is indeed very easy to find linear features in man-made environments and record them in several images to assess the repeatability of estimation. The distortion coefficients are introduced as unknowns in a process of straight line fitting to image lines, which must be well distributed over the frame. The equation for each line will be one of the following two (according to line slope):

$$x - \Delta x + t(y - \Delta y) + b = 0 \qquad t(x - \Delta x) + y - \Delta y + b = 0 \tag{3}$$

It is noted that here it is impossible to find a coefficient k_o for the linear term in Eq.1. From this approach results have already been reported for wide-angle lenses of a small format camera (Karras et al., 1998). Various other cameras have been tested since (Routsis, 2000; Kallianou, 2001). Typical small format images used in these tests are seen in Fig. 5. In general, a satisfactory repeatability has been established, provided that image lines are well distributed. In Fig. 6 an example of a medium format camera is given.

Figure 5: Small-format images from different lenses (three with f = 17 mm, one with f = 24 mm) used for estimation of distortion

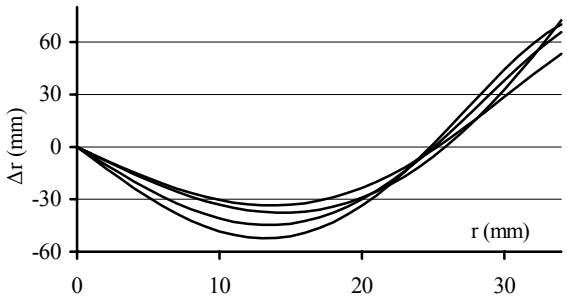

Figure 6: Above: two images form a Fuji 45x60 mm^2 camera with lens f = 45 mm; right: distortion curves from four images

Besides repeatability, however, the performance of the approach should also be practically tested as regards accuracy. Distortion data from lines were introduced into two of the previous examples, yielding the results of Table 3.

Table 3. Results with correction of Δr from lines (cf. Table 2)

Project	RMS of control points (cm)		
	X	Y	Z
"Sparta"	1.4	1.0	2.5
"Thisseio"	3.8	4.6	3.1

Compared to those of Table2, these results show that in the second case radial distortion has been fully recovered from line-fitting. It is equally clear, however, that in the first case the main part of Δr has also been corrected but a certain loss of accuracy in depth is present, which indicates the limitations of the approach. Line-fitting cannot totally replace rigorous camera calibration. Finally, as already mentioned, distortion thus estimated can also allow correction of digital images. In Fig. 7 two such examples are given.

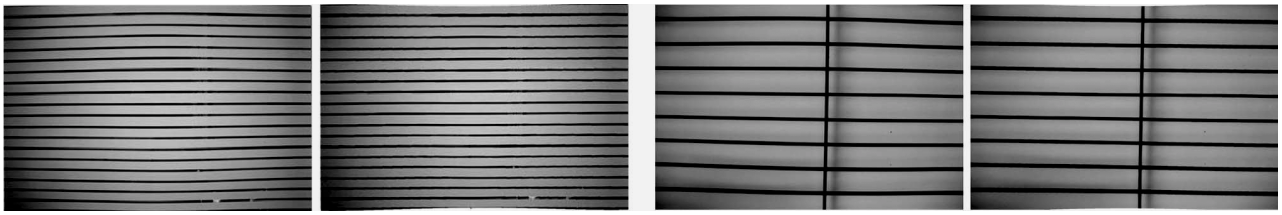

Figure 7: Images before and after correction of distortion. Left: Tokina lens (f = 17 mm). Right: Soligor lens (f = 24 mm)

3.2 Estimation of distortion with the rectification of regular grids

Since radial symmetric lens distortion is, in principle, the largest among image errors, its consequences are often clear in rectification results, especially where regular grids covering most of the frame are concerned. In Fig. 8 such an example is given showing how the correction of distortion reduces drastically the image residuals in x and y. In fact, the first two pictures unmistakably reveal a typical distortion pattern, with large errors near the frame corners followed by negligible distortion at a certain radius and then larger errors with opposite sign (here only the absolute values of residuals are seen) which finally disappear around the centre. Consequently, it is possible to exploit the rectification of regular grids for estimating distortion.

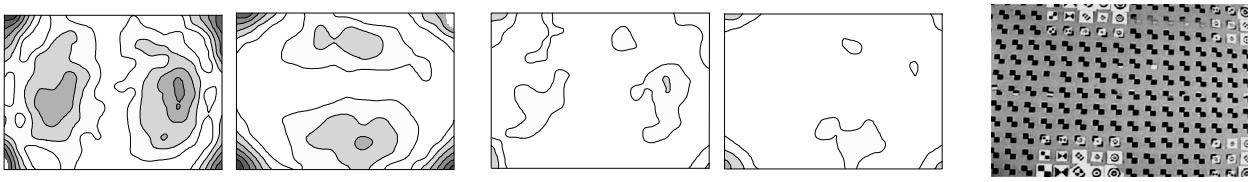

Figure 8: Distribution of image residuals in x and y after the rectification of a Nordmende video frame of a regular grid. Left: with measured image coordinates. Centre: with image coordinates corrected from Δr. Right: the video frame.

A most direct approach would be to directly introduce the coefficients of the distortion polynomial as unknowns into the rectification algorithm. The 2D-2D projective equations can then take the following linear form:

$$x - \Delta x + v_x = a_{11}x + a_{12}y + a_{13} - a_{31}xX - a_{32}xY \qquad y - \Delta y + v_y = a_{21}x + a_{22}y + a_{23} - a_{31}yX - a_{32}yY \tag{4}$$

in which Δx, Δy denote the Δr components as in Eq. 2. Two points need to be stressed here. First, that the image measurements may, of course, be in pixel dimensions but, contrary to other applications of projective equations, they must necessarily refer to the image centre. Second, that only terms k_1 and k_2 of Eq. 1 can be used since the scale is taken into account by the projective coefficients.

3.2 Estimation of distortion from the rectification residuals

Although the approach just outlined is more rigorous, radial distortion may also be estimated by fitting Eqs. 2 to the x and y residuals of a conventional rectification (which are obtained when using Eq. 4 without the Δx, Δy terms). Such an approach could be more useful to several users since its programming is easier. But even for those who simply use available software, most commercial rectification modules include image residuals in their output. These can then be plotted against the grid in some graphics environment to convey to the user an idea about the magnitude and distribution of distortion. An example is given in Fig. 9.

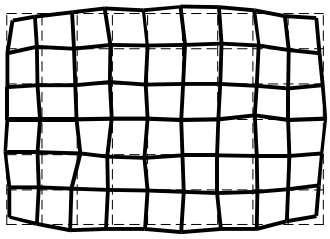

Figure 9: Distribution of residuals on the image after rectification of a regular grid recorded with a Mamiya 60x90 mm^2 camera and a normal lens (f = 100 mm). Though contaminated with relatively large measuring errors, the distortion pattern is rather clear. Residuals have been enlarged here 30 times.

3.2 Estimation of distortion from the residuals of partial rectification

There are instances where only one of the two space X, Y coordinates of points of a planar object are known, notably when the image depicts parallel lines assumed to be equidistant. For example, points on a vertical line will have the same X coordinate (say, X = 0) and, if the equidistance is given an arbitrary value d, points on the next line will all have X = d, those on the third X = 2d etc. Here, a

simple approach to estimate distortion would be to use only one of the inverse relations of Eq. 4, "pretending" that now the space coordinate suffer from distortion with opposite sign, expressed in their residuals v_X (or, for horizontal lines, v_Y):

$$X + v_X = b_{11}X + b_{12}Y + b_{13} - b_{31}Xx - b_{32}Xy \qquad \text{or} \qquad Y + v_Y = b_{21}X + b_{22}Y + b_{23} - b_{31}Yx - b_{32}Yy \tag{5}$$

Assuming nearly-frontal recording of the planar object (small camera tilt), the first coefficient of the left and the second of the right equation basically describe the scale of the image, if affinity is ignored. Thus, the corresponding image residuals can be estimated as:

$$v_x = -\frac{v_X}{b_{11}} \qquad \text{or} \qquad v_y = -\frac{v_Y}{b_{22}} \tag{6}$$

These image residuals may be used either to estimate distortion according to 3.2 using the corresponding equation of Eq. 2 or simply to visualise it. This approach is given here as simpler than line-fitting, but generally it will be less precise than the previous ones as it uses information only from one direction assuming radial symmetry. However, it could provide satisfactory results, particularly for lenses with significant distortion, as in the examples given in Fig. 10 where results are compared to those from line-fitting. It is noted that in the case on the right only the three, though well-distributed over the negative, horizontal lines have been used.

Figure 10: Distortion curves for two images of the same lens from line-fitting and from fitting to partial rectification residuals

The approaches outlined in this section provide relatively simple tools for the estimation of radial distortion. Although such "partial calibrations" might suffice for several applications, particularly of moderate accuracy requirements, there are instances where a more rigorous process, i.e. full camera calibration, is needed. Probably the easiest approach would be through the use of planar test-fields.

4 MULTI-IMAGE CALIBRATION WITH PLANAR TEST-FIELDS

Indeed, among the alternatives discussed in the Introduction planar test-fields may provide a good alternative. Depending on viewing angle of the camera and imaging distance, such planar grids could be either generated with a plotter for close-range recording or constructed, if larger dimensions are required; however, even for the second case suitable grid-like patterns are also to be found in man-made environments. Evidently, such solutions represent a multi-mage approach. The combined images are assumed to have identical inner orientation and must have been acquired with significant tilts to produce strongly differing perspective views of the plane. Two examples of digital cameras will be given here to illustrate two different cases.

An Agfa digital camera, focused at 2 m, was used to record a targeted 10 cm x 10 cm grid from several viewing angles (see Fig. 11). Results for bundle adjustments with different image combinations are given in Table 4 and Fig. 12 (Kossovas and Mourafetis, 2000).

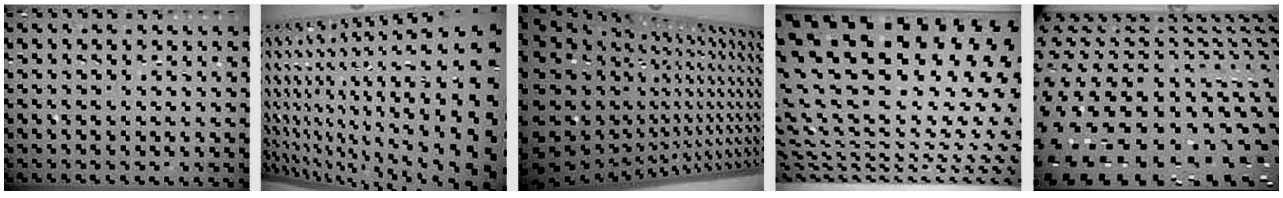

Figure 11: Images of a targeted planar grid taken with an Agfa digital camera.

Table 4. Self-calibration results from a planar grid (Agfa camera)

Number of Images	7	8	9	10
c_x (pixel)	1854.3	1852.6	1854.8	1851.3
$c_x : c_y$	0.9999	0.9996	0.9998	0.9994
x_o (pixel)	4.3	4.3	3.6	3.8
y_o (pixel)	-5.8	-6.3	-7.1	-7.3

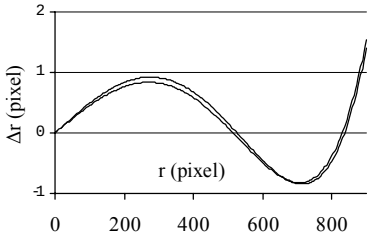

Fig. 12. Δr curves from two self-calibration solutions

These results, based on all available 256 points, show a high consistency. Furthermore, affinity (c_x:c_y) is very small, while the shift of the principal point from the image centre as well as lens distortion are also relatively limited. Actually, all these parameters could be neglected in several practical situations.

But this is not true for the camera of the next example, a Pulnix digital camera. All five very close-range images, seen in Fig. 13, and the measurements have been downloaded from a Web site (Zhang, 1998). The grid covers a total area of 17 x 17 cm^2 and had been recorded from imaging distances of about 35 cm. The results are given in Table 5 (Kossovas and Mourafetis, 2000).

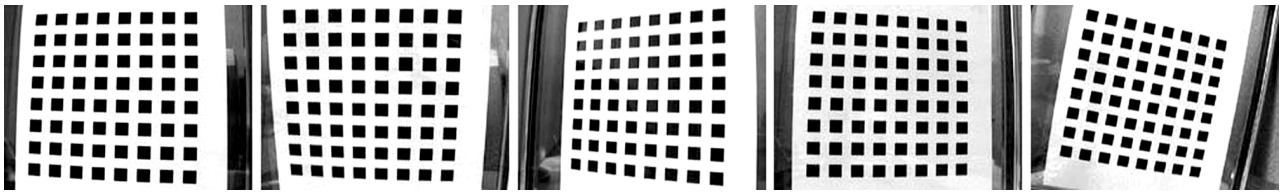

Figure 13: Images of a targeted planar grid taken with a Pulnix digital camera (Zhang, 1998).

Table 5. Self-calibration results from a planar grid (Pulnix camera)

Number of Images	3	4	5
c_x (pixel)	834.3	834.2	834.0
c_y (pixel)	834.2	834.2	834.0
x_o (pixel)	16.7	16.8	16.7
y_o (pixel)	-35.2	-35.0	-35.2

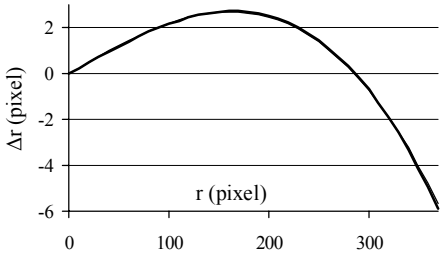

Fig. 14. Δr curves from self-calibration with 5 images and from rectification of the first image

The above results, too, display a high consistency. In fact, given the large distortion of the lens and the high precision of measurements, the curves coincide with those estimated from rectification (Fig. 14). Affinity, furthermore, is negligible. Nevertheless, the large displacement of the principal point from the centre cannot be overlooked. Particularly in the vertical direction, this shift exceeds 7% of the 640x480 frame size (i.e. is equivalent to ~2 mm in a 35 mm camera). Generally, unless projective equations are adopted or the object has a very limited extension in depth, such displacements of the principal point cannot be neglected. To verify this, further self-calibration adjustments were carried out with the same images, based on 12 control and 52 tie points (Kalisperakis and Tzakos, 2001). The results are given in Table 6.

Table 6. Self-calibration results form 5 Pulnix images of a planar grid (12 control points)

Adjustment	RMS of 52 tie points (mm)		
	X	Y	Z
full self-calibration	0.03	0.04	0.06
self-calibration ignoring Δr (= 0)	0.28	0.31	0.08
self-calibration ignoring x_o, y_o (= 0, 0)	0.13	0.12	0.07
self-calibration with Δr given from 3.1	0.03	0.04	0.06
self-calibration with Δr given from 3.2	0.03	0.04	0.06
self-calibration with Δr given from 3.3	0.07	0.09	0.06
self-calibration with Δr given from 3.4 (in X)	0.09	0.11	0.06
self-calibration with Δr given from 3.4 (in Y)	0.05	0.07	0.06

One sees in the first rows of Table 6 that, although distortion evidently remains by far the most important source of inaccuracy, errors are trebled in two directions when the principal point is not taken into account. Hence, ignoring the principal point would lead here to significant errors, especially if large extension in depth is present. Apparently, this has chiefly to do with the error introduced directly into the adjustment by the omission of x_o, y_o and not with the fact that in this case distortion has a different point of best symmetry (it is expressed radially about the image centre rather than the principal point). This is observed in the last five rows of Table 6, in which distortion curves for the first image only (referring to its centre) had been estimated prior to adjustments via the described methods. In fact, the distortion polynomials estimated both from line-fitting and rectification gave RMS values identical to those of full bundle adjustment, while the simpler approaches led to less accurate solutions in which, nonetheless, distortion has been largely corrected.

5 FINAL REMARKS

Purpose of this contribution was to discuss aspects of interior orientation, a crucial photogrammetric problem which often embarrasses users and is a source of serious errors. In the context of a growing demand for photogrammetric products in architecture and archaeology which are mainly based on non-metric cameras, approaches possibly simple have been addressed here, illustrated with

examples from practical applications. Yet, this discussion started with cases in which "nominal" values for interior orientation would meet a moderate accuracy requirement, and ended up with an example showing the consequence of ignoring the principal point. Interior orientation is in principle a complicated issue, and "conclusions" cannot be drawn easily. Instead, two remarks could be founded on the experiences presented here.

- A first remark concerns what has been termed "nominal" values for interior orientation. It has been shown here that, for several practical cases with analogue cameras, use of these values would lead to acceptable results. No particular tolerances can be given for all instances, but it is rather clear that in this case the extension in depth of the object plays the important role.
- Radial-symmetric lens distortion, on the other hand, does not fall into the same category. It has been illustrated that its effects can be very important (regardless of object), and simple methods have been outlined for its estimation. Our experience indicates that such techniques can grasp and correct, at least up to a certain extent, a main component of distortion and allow a considerable increase in accuracy. These methods can also be valuable in cases where interior orientation is otherwise irrelevant, notably in rectification.

Further possible alternatives for moderate or low accuracy requirements need also be investigated. For instance, when focusing is not at infinity one is often tempted to simply apply the well-known equation of thin lenses in order to estimate the principal distance (camera constant). To which extent would this be a "legitimate" choice? Other questions also remain unclear. For instance, does it actually matter if we simply ignore the point of best symmetry and refer distortion to the principal point, or even the image centre? Or: may one assume distortion as being constant for all focusing distances? And for all lenses of the same type? Similar questions are to be addressed in the future.

Finally, a rough distinction should be made between analogue and digital (or video) cameras. One might say that analogue cameras generally display a "predictable" behaviour. Digital cameras, on the other hand, have introduced certain parameters hitherto marginal in photogrammetric practice, e.g. large displacements of the principal point, considerable affine deformations, extensive use of zoom lenses etc. From this point of view, digital cameras basically need a somewhat different treatment. Of course, these problems are irrelevant in certain cases (such as in the popular technique of rectification). But the fact remains that lenses are still subject to distortion, which could be corrected with simple methods like the ones discussed in this contribution.

REFERENCES

Bieler, M., Höpfner, H., Mundt, D., 2001. Vermessung einer byzantinischen Kapelle in Athen. Diploma Thesis, Department of Surveying, University of Applied Sciences, Berlin, pp. 103.

Galinou, R., Katsali, E., 1999. Investigation of the influence of interior orientation errors on photogrammetrically determined object space coordinates. Diploma Thesis, Department of Surveying, National Technical University of Athens, pp. 268. (In Greek.)

Kalisperakis, I., Tzakos, A., 2001. Development of a self-calibrating bundle adjustment software in the AutoCad environment. Diploma Thesis, Department of Surveying, National Technical University of Athens, pp. 180. (In Greek.)

Kallianou, F., 2001. A simple method for determining radial distortion in analogue and digital cameras. Diploma Thesis, Department of Surveying, The Technological Educational Institute of Athens, pp. 167. (In Greek.)

Karras, G. E., Mountrakis, G., Patias, P., Petsa, E., 1998. Modeling distortion of super-wide-angle lenses for architectural and archaeological applications. International Archives of Photogrammetry & Remote Sensing, vol. 32, Bd. 5, pp. 570-573.

Karras, G. E., Mavromati, D., Madani, M., Mavrellis, G., Lymperopoulos, E., Kambourakis, A., Gesafidis, S., 1999. Digital orthophotography in archaeology with low-altitude non-metric images. International Archives of Photogrammetry & Remote Sensing, vol. 32, Bd.. 5W11, pp. 8-11.

Kölbl. O. R., 1976. Metric or non-metric cameras. Photogrammetric Engineering and Remote Sensing, vol. 42, no. 1, pp.103-113.

Kossovas G., Mourafetis, G., 2000. Multi-image calibration of digital cameras using planar testfields. Diploma Thesis, Department of Surveying, National Technical University of Athens, pp. 292. (In Greek.)

Petsa, E., 2001. Photogrammetric survey of the parodos walls of the Ancient Theatre of Sparta. Technical Report, Department of Surveying, The Technological Educational Institute of Athens, pp. 12.

Routsis, E., 2000. Determination of lens distortion from images of straight lines. Diploma Thesis, Department of Surveying, National Technical University of Athens, pp. 257. (In Greek.)

Zhang, Z., 1998. A flexible new technique for camera calibration. Microsoft Research Technical Report MSR-TR-98-71, Microsoft Corporation, pp. 21 (http://research.microsoft.com/~zhang)